Picosecond transient grating spectroscopy: The nature of the diffracted spectrum

Claudia Högemann, Marc Pauchard, and Eric Vauthey
Institute of Physical Chemistry of the University of Fribourg, Pérolles, CH-1700 Fribourg, Switzerland

(Received 28 May 1996; accepted for publication 28 June 1996)

A ps transient grating setup using white light continuum for probing is presented. Measurements on an aromatic molecule in solution have been carried out with this system. The diffracted spectrum is analyzed using Kogelnik's coupled wave theory. At short time delay after excitation, the diffracted spectrum is strongly dominated by absorption and in this case transient grating spectroscopy is equivalent but more sensitive to transient absorption spectroscopy. If some of the excitation energy is dissipated as heat, the diffracted spectrum is essentially the same as the dispersion spectrum of the transient species at time delays approaching half the acoustic period. The performances of this technique and of transient absorption spectroscopy are compared. © *1996 American Institute of Physics.* [S0034-6748(96)00910-0]

I. INTRODUCTION

Over the past decade, the transient grating (TG) technique has been intensively applied to the study of many physical processes[1] such as electronic energy transport,[2,3] studies of diffusion in liquids,[4] optical Kerr effect,[5,6] excited state dynamics,[7,8] rotational diffusion dynamics,[9,10] and photoinduced electron transfer.[11] In a transient grating experiment, the sample is excited by two spatially crossed and time coincident laser pulses producing an interference pattern. Interaction between the light field and the sample will result in a spatially modulated complex refractive index of the sample in the crossing region. The amplitude of this grating like distribution is measured by a third time delayed laser pulse striking the grating at Bragg angle. The intensity of the diffracted light depends on the modulation amplitude of the complex refractive index grating, i.e., on the variation of absorbance and refractive index in the sample. Therefore, TG can be used as an alternative to the more conventional transient absorption spectroscopy. As the TG signal has a zero background, this technique is much more sensitive than transient absorption and requires less pump light intensity. The superior sensitivity of grating detection over transmission has been very clearly demonstrated in spectral hole-burning spectroscopy by Wild and co-workers.[12,13] Until recently, grating detection was performed with laser light and therefore a diffracted spectra over only a relatively small range could be obtained by tuning the laser wavelength.[14–18] The lack of transient diffracted spectra over a larger wavelength range is, of course, a major drawback of TG over transient absorption. TG has been successfully applied to study the energetics of photoinduced reactions as well as the dynamics of heat releasing processes.[19–21] In order to analyze the TG data correctly, knowledge of the diffracted spectrum as well as the extent of interaction between population and density phase gratings is of great importance. Recently, Masuhara and co-workers presented transient diffracted spectra of benzophenone[22] as well as of copper phtalocyanine film[23] measured by fs TG using white light continuum for probing. The authors conclude that in the short time scale investigated, the diffracted spectra were essentially the same as the absorption spectra.

In this article, we present a study of the nature of the diffracted spectrum obtained in ps TG spectroscopy with white light continuum. We have particularly investigated the contribution of absorption and dispersion spectra to the diffracted spectrum at short time delay and also at longer time delay where the influence of acoustic waves due to heat releasing processes becomes important.

II. EXPERIMENT

A. Apparatus

The TG setup is depicted in Fig. 1. The third harmonic output at 355 nm of an active/passive mode-locked *Q*-switched Nd:YAG laser with a single amplification stage (Continuum PY61-10) was split in two parts, which, after traveling through different paths of the same length, recombined on the sample with an angle of incidence of 0.4°. The duration of the pulses was about 30 ps and the pump energy on the sample was around 500 μJ. The diameter of the spot on the sample was around 3 mm and was adjusted with a set of two 500 mm focal length lenses. To ensure a perfect time coincidence between the two pump pulses, one of them was deviated along a short adjustable optical delay line. The polarization orientation of both pulses was set at 54.75° relative to the vertical with a combination of half-wave plates and polarizers. The remaining laser output at 1064 nm was sent along a variable optical delay line, consisting of a corner-cube retroreflector on a motorized translation stage, before being focused with a 300 mm focal length lens in a 25-cm-long quartz cell filled with water to generate a with light continuum between 450 and 750 nm. The white light pulses were spatially filtered, then passed through a vertical polarizer and were focused on the sample to a spot of about 2 mm diameter with an angle of incidence of 0.7°. Each wavelength component of the continuum is Bragg diffracted at a different angle and with an efficiency which depends on the complex refractive index spectrum of the photogenerated species. This dispersed signal was passed though a cutoff filter (Schott GG400) to eliminate scattered pump light. It was then recombined with a prism and focused in a light guide connected to the entrance of a 1/4 m imaging spectrograph (Oriel Multispec 257) equipped with a 300

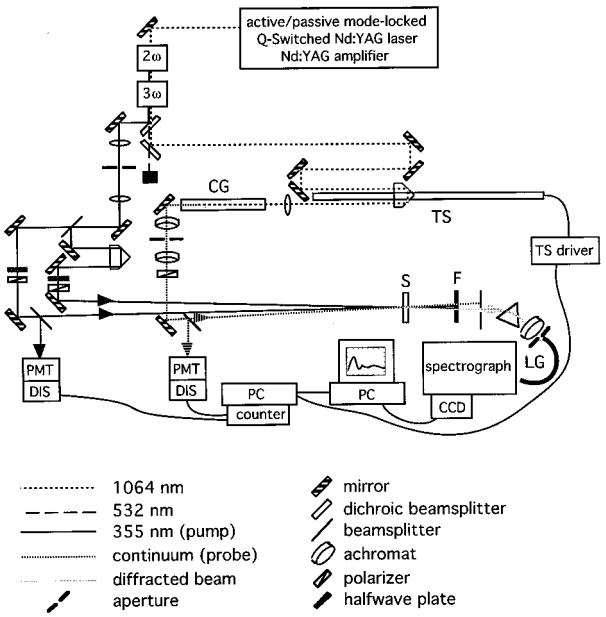

FIG. 1. Picosecond transient grating setup (CG: water cell for continuum generation, TS: translation stage, S: sample; F: cutoff filter, LG: light guide, PMT: photomultiplier tube, DIS: discriminator).

grooves/mm grating. As detector, a 1024×256 pixels water cooled charge coupled device (CCD) camera (Oriel Intaspec IV) was used.

B. Data acquisition

The intensity of a fraction of one pump pulse and of the white light pulse was monitored by two photomultiplier tubes. Both output signals were sent into two discriminators, whose levels were set to allow only laser pulses within a small intensity range to generate a transistor–transistor logic (TTL) signal. The occurrence of these signals was checked with a counter PC board (Metrabyte CTM-05). The status of this counter was interrogated after the acquisition of each single shot spectrum. If the counts were smaller than two, the single shot spectrum was discarded. This sequence was repeated until 50 good shots were obtained. This corresponds to an acquisition time of about 30 s. Diffracted spectra were obtained by first subtracting the background spectrum, which was measured when probing 100 ps before excitation. This spectrum contained a small fraction of scattered continuum and in some cases some fluorescence from the sample. The ensuing spectrum was corrected for the spectral shape of the probe light through division by the white light continuum spectrum. Probing with slightly different angles (±0.2°) did not affect the shape of the diffracted spectrum.

C. Samples

9,10-Dicyanoanthracene (DCA Kodak) was sublimed twice under vacuum, anisole (Fluka) was purified as described in Ref. 24. Acetonitrile (MeCN, Fluka) was of spectroscopic grade and used as such. The absorbance of the sample solutions at 355 nm was between 0.1 and 0.2 on 1 mm, the sample thickness. All experiments were performed at 20±1 °C.

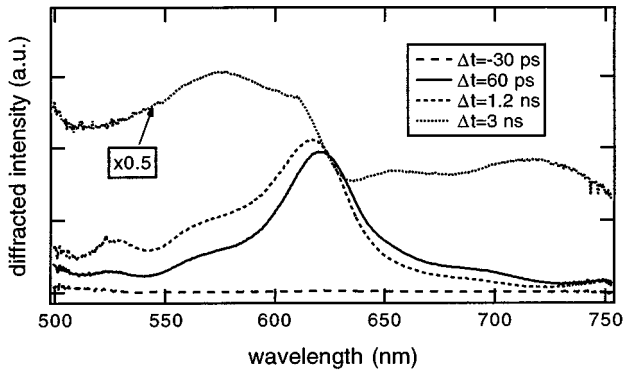

FIG. 2. Diffracted spectra measured at various time delays after excitation of a solution of DCA in MeCN.

III. RESULTS AND DISCUSSION

Figure 2 shows the diffracted spectrum of DCA in MeCN measured at different time delays after excitation at 355 nm. This spectrum is ascribed to a DCA S_1 state which has a lifetime of about 15 ns and a fluorescence yield of 0.9.[25] After the initial growth, the shape of the band remains unchanged for about 1 ns. As the time delay becomes longer, the intensity of the diffracted spectrum increases strongly and the spectral shape changes substantially. In order to understand the origin of this effect, the nature of the diffracted spectrum has to be considered. The diffraction efficiency of a grating, η, defined as the ratio of the intensities of the diffracted, I_{dif}, and incident probe pulses, I_{inc}, can be calculated according to Kogelnik's coupled wave theory[26] as

$$\eta(\omega,t)=\left[\sinh^2\left(\frac{\alpha_1(\omega,t)d}{2\cos\theta}\right)+\sin^2\left(\frac{\beta_1(\omega,t)d}{2\cos\theta}\right)\right]\times\exp\left(-\frac{2\alpha_0(\omega,t)d}{\cos\theta}\right), \tag{1}$$

where $\alpha_1(\omega,t)$ is the amplitude of the modulation of the amplitude absorption coefficient, $\beta_1(\omega,t)$ is the modulation amplitude of the propagation constant, $\alpha_0(\omega,t)$ is the average amplitude absorption coefficient, θ is the Bragg angle, and d is the sample thickness. The first term in brackets describes the amplitude grating and the second the phase grating. The exponential term accounts for the attenuation of the diffracted light intensity by the sample. The factor of 2 results from using the amplitude absorption coefficient. The terms $\alpha_1(\omega,t)$ and $\beta_1(\omega,t)$ are the first Fourier coefficients of the series expressing the spatially periodic variation of $\alpha(\omega,t)$ and $\beta(\omega,t)$. As long as the excitation intensity is not too high, these modulations are harmonic and higher order terms, responsible for second and higher order diffraction, can be neglected. The modulation amplitude $\alpha_1(\omega,t)$ is given by

$$\alpha_1(\omega,t)\cong\Delta\alpha(\omega,t)=\frac{2\pi}{\lambda}\Delta k(\omega,t)$$

$$=\sum_i 1.15\cdot\epsilon_i(\omega)\cdot\Delta C_i(t), \tag{2}$$

where $\Delta k(\omega,t)$ is the change of the attenuation index, λ is the probe wavelength, and ΔC_i the change of concentration of the component i with an extinction coefficient ϵ_i. Similarly, $\alpha_0(\omega,t)$ is expressed as

$$\alpha_0(\omega,t)=1.15\cdot A(\omega,t)/d, \tag{3}$$

$A(\omega,t)$ being the absorbance of the sample. The modulation amplitude of the propagation constant is defined as

$$\beta_1(\omega,t)\cong\frac{2\pi}{\lambda}\,\Delta n(\omega,t)=\Delta n_p(\omega,t)+\Delta n_d(\omega,t), \tag{4}$$

where $\Delta n(\omega,t)$ is the total change of refractive index which is the sum of the variation of refractive index related to changes of population, $\Delta n_p(\omega,t)$, and to variation of density, $\Delta n_d(\omega,t)$. The latter is mainly caused by thermal expansion following heat releasing processes, such as nonradiative transitions or exothermic reactions.

The time evolution of $\Delta n_d(\omega,t)$ depends on the acoustic period, the τ_{ac}, i.e., the time needed for the illuminated fringe to reach its new density. This parameter depends on the size of the fringe, Λ, and on the speed of sound, ν_s,[27]

$$\tau_{ac}=\frac{\Lambda}{\nu_s}=\frac{\lambda_e}{2\sin\theta_e\cdot\nu_s}, \tag{5}$$

λ_e being the wavelength of the excitation pulses with an angle of incidence θ_e. If heat is released within a time shorter than this period, the diffracted intensity due to the thermal phase grating exhibits a sinusoidal oscillation between zero and a maximum value with a period of τ_{ac}. With the geometry used in these experiments, τ_{ac} amounts to about 20 ns. At short time delays, $\Delta t<1$ ns, the total variation of refractive index is therefore only due to the change of refractive index related to population, $\Delta n_p(\omega,t)$.

For small diffraction efficiencies, $\eta<10^{-2}$, the sin and sinh functions in Eq. (1) can be replaced by their arguments. With this approximation and using Eqs. (2)–(4), Eq. (3) can be rewritten as

$$\eta(\omega,t)\cong\exp\left(-\frac{2.3A(\omega,t)}{\cos\theta}\right)\left(\frac{\pi d}{\lambda\cos\theta}\right)^2 \times[\Delta k^2(\omega,t)+\Delta n^2(\omega,t)]. \tag{6}$$

This expression shows that a diffracted spectrum is proportional to the sum of the squares of the absorption and dispersion spectra of the species produced upon excitation. Considering the very small concentration of the photogenerated species, the first term of Eq. (6) is only significant in the regions where the unexcited sample absorbs.

It is well known that the absorption and dispersion spectra are connected through the Kramers–Kronig relation,[28] and therefore each spectrum can be converted into the other through the Hilbert transformation

$$n(\omega)=-\frac{1}{\pi}\int_{-\infty}^{+\infty}\frac{k(\omega')}{\omega-\omega'}\,d\omega'. \tag{7}$$

Figure 3(A) shows the diffracted spectrum of DCA in MeCN measured 60 ps after excitation together with a calculated spectrum. The latter was obtained as follows: the absorption spectrum, $k(\omega)$, was built up as the sum of six Gaussian functions with adjustable center position, width, and intensity. The dispersion spectrum, $n(\omega)$, was then calculated using the Hilbert transformation. The sum of the square of both spectra was fitted to the measured diffracted spectrum using the Marquardt–Levenberg nonlinear least-square method. Figure 3(B) displays the calculated absorption and dispersion spectra and their contribution to the diffracted spectrum is shown in Fig. 3(C). It is immediately clear that the general shape of the absorption and diffracted spectra are very similar. The main difference is the larger width of the band in the diffracted spectrum, due to the contribution of dispersion at the edges.

In order to explain the shape of the diffracted spectrum measured at longer time delay ($\Delta t=3.5$ ns) shown in Fig. 2, the variation of refractive index coupled to change of den-

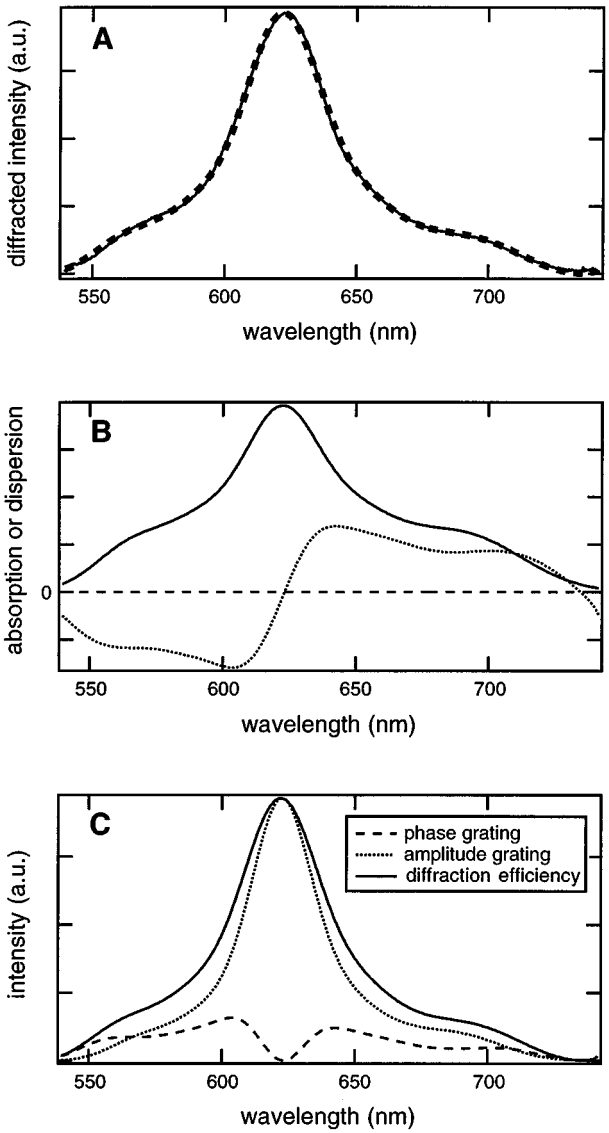

FIG. 3. (A) Fit (dotted line) of the diffracted spectrum measured at short time delay (solid line). (B) Absorption (solid line) and dispersion (dotted line) spectra obtained from the fit. (C) Contribution of absorption and dispersion to the diffracted spectrum.

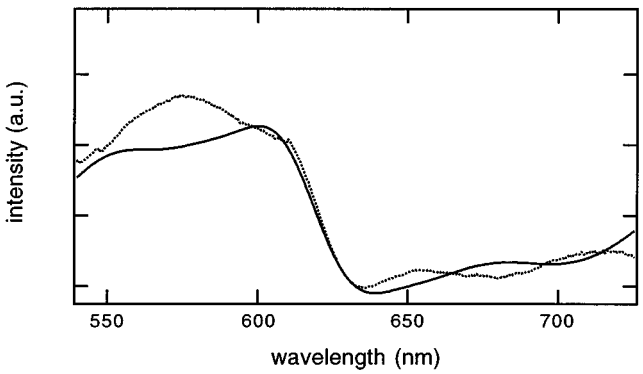

FIG. 4. Comparison of the diffracted spectrum measured at long time delay (dotted line) with the negative of the dispersion spectrum (solid line).

sity, $\Delta n_d(\omega,t)$, has to be taken into account. In this case, the diffraction efficiency is proportional to

$$\eta(\omega,t) \propto \Delta k^2(\omega,t) + \Delta n_p^2(\omega,t) + \Delta n_d^2(\omega,t) + 2\Delta n_p(\omega,t)\Delta n_d(\omega,t), \tag{8}$$

where both phase grating components interfere through the cross term.[29] The energy of the S_1 state of DCA amounts to 2.88 eV. After excitation at 355 nm, 0.62 eV of energy are released as heat within a few ps. As the probe delay approaches 10 ns ($\tau_{ac}/2$), $\Delta n_d(\omega)$ becomes much larger than $\Delta n_p(\omega)$ and $\Delta k(\omega)$ and the first two terms on the right-hand side of Eq. (8) can be neglected. In this case, the shape of the diffracted spectrum depends on the wavelength dependence of Δn_p and Δn_d. The spectrum of the latter term is essentially the same as the dispersion spectrum of the nonexcited sample. In the spectral window investigated, i.e., between 450 and 750 nm, Δn_d decreases smoothly from the blue to the red wavelengths. This has been verified by measuring the diffracted spectrum at long time delay ($\Delta t \approx 2$ ns) with a solution of 2-hydroxybenzophenone in acetonitrile. After excitation, this molecule undergoes a very fast relaxation to the ground state by reversible intramolecular proton transfer releasing the whole excitation energy as heat. Its diffracted spectrum at $\Delta t > 1$ ns is due to $\Delta n_d(\omega)$ only, as the population gratings have decayed in a few ps.

Coming back to DCA at long time delays, the diffracted spectrum is therefore composed of a smooth background due to the third term of Eq. (8) and of the dispersion spectrum related to population multiplied by $\Delta n_d(\omega,t)$. As this term is smaller than zero and has a weak wavelength dependence, the shape of the diffracted spectrum must be almost identical to the reverse of the dispersion spectrum, i.e., to $-\Delta n_p(\omega,t)$. Figure 4 compares the diffracted spectrum measured at large time delay ($\Delta t = 3.5$ ns) with the dispersion spectrum obtained from the fit of the diffracted spectrum observed at short time delay ($\Delta t = 60$ ps). It can be seen that the agreement is very good on the long wavelength side of the band. The difference observed on the blue side originates probably from the spectral shape of Δn_d, which is larger at shorter

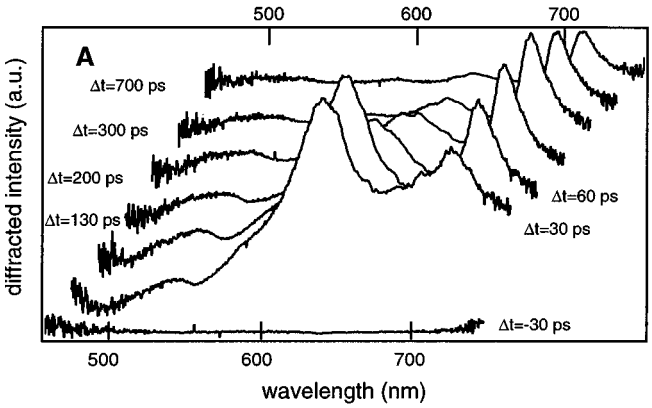

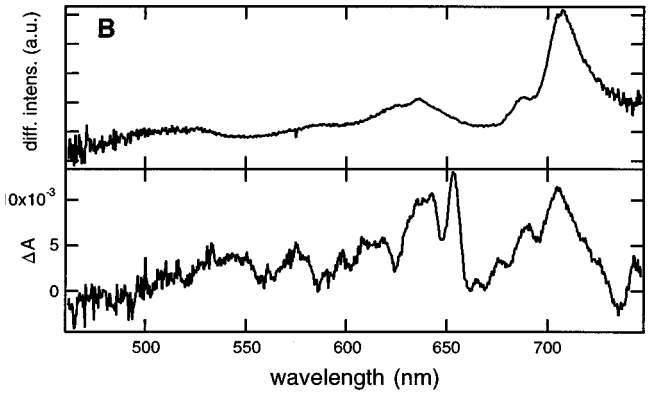

FIG. 5. (A) Diffracted spectra measured at various time delays after excitation of a solution of DCA with 0.5 M anisole in MeCN. (B) Diffracted spectrum (top) and transient absorption spectrum (bottom) of the same solution as in (A) measured 250 ps after excitation with the same experimental conditions.

wavelengths. The presence of a new species formed at longer time delays, such as ^{3}DCA* could additionally be at the origin of this discrepancy.

With the geometrical arrangement use in these experiments, the transformation of the shape of diffracted spectrum starts from a time delay superior to 1 ns. From here, the intensity of the red side of the band decreases, while the intensity on the blue side increases (see Fig. 2). This effect comes from the relative signs of Δn_d and Δn_p. As mentioned earlier, the thermoinduced change of refractive index is negative. On the red side of the absorption band of DCA*, Δn_p is positive and both phase grating interfere destructively through the cross term of Eq. (8). On the blue side of the band, both Δn_d and Δn_p are negative, and the grating interferes constructively, leading to an augmentation of the diffraction efficiency. At the band maximum, Δn_p is zero and no interference can take place. This transformation takes place until Δn_d becomes larger than the other terms of Eq. (8), where the spectrum shown in Fig. 4 is obtained. The time from which this modification develops can be delayed by diminishing the angle of incidence of the pump pulses. With a small enough angle, the interference with the density phase grating can be eliminated up to a time delay of 5 ns. In these conditions, TG spectroscopy with white light con-

tinuum is a very valuable alternative to transient absorption spectroscopy. For example, Fig. 5(A) show the diffracted spectra measured at various time delays after excitation of a solution of DCA with 0.5 M anisole in MeCN. As the time delay is increased, the band related to ^{1}DCA* located around 620 nm decays because of electron transfer quenching. In parallel, a band around 700 nm corresponding to $DCA^{\cdot -}$ (Ref. 30) builds up to a maximum and decreases to an intensity which stays constant on the ns time scale. This behavior reflects the competition between back electron transfer to the neutral ground state and dissociation into free ions.[31] For these spectra the angle of incidence of the pump pulses was 0.15°. The decrease of diffraction efficiency upon deviation from the Bragg angle is negligible in view of this small angle. Indeed, the spectral half power bandwidth of the grating, $\Delta\lambda_{1/2}/\lambda \approx \cot\theta(\Lambda/d)$,[26] is much larger than the spectral width of the white light continuum.

Figure 5(B) shows a comparison of the transient absorption spectrum and of the diffracted spectrum recorded with the same pulse energies and acquisition parameters. It is immediately clear that the signal-to-noise ratio is by far superior with TG detection. The bands observed in the diffracted spectrum can be found in the absorption spectrum, but with a different intensity ratio. This is due to the quadratic dependence of the TG signal on concentration changes. Many of the small features in the absorption spectrum are not real and are due to the weakness of absorbance changes. A variation of optical density smaller than 0.01 results in a very good diffracted spectrum. This result also confirms the assumption made above that the first term of the right-hand side of Eq. (6) can be neglected at wavelengths where the unexcited sample does not absorb.

The TG technique allows the detection of transient species with low extinction coefficients without too high excitation intensities, at which undesired nonlinear optical processes can occur.

ACKNOWLEDGMENTS

This work was supported by the Fonds National Suisse de la Recherche Scientifique through Project No. 20-41855.94 and by the Programme d'encouragement à la Relève Universitaire de la Confédération. Financial support form the Fonds de la Recherche and the Conseil de l'Université de Fribourg is also acknowledged.

[1] H. J. Eichler, P. Günter, and D. W. Pohl, *Laser-Induced Dynamic Gratings* (Springer, Berlin, 1986).
[2] J. R. Salcedo, A. E. Siegman, D. D. Dlott, and M. D. Fayer, Phys. Rev. Lett. **41**, (1978).
[3] L. Gomez-Jahn, J. Kasinski, and R. J. D. Miller, Chem. Phys. Lett. **125**, 500 (1986).
[4] M. Terazima, Chem. Phys. Lett. **218**, 572 (1994).
[5] G. A. Kenney-Wallace and S. Wallace, IEEE J. Quantum Electron. **QE-19**, 719 (1983).
[6] F. W. Deeg, J. J. Stankus, S. R. Greenfield, V. J. Newell, and M. D. Fayer, J. Chem. Phys. **90**, 6893 (1989).
[7] D. W. Phillion, D. J. Kuizenga, and A. E. Siegman, Appl. Phys. Lett. **27**, 85 (1975).
[8] E. Vauthey, Chem. Phys. **196**, 569 (1995).
[9] R. S. Moog, M. D. Ediger, S. G. Boxer, and M. D. Fayer, J. Chem. Phys. **86**, 4694 (1982).
[10] E. Vauthey, Chem. Phys. Lett. **216**, 530 (1993).
[11] E. Vauthey and A. Henseler, J. Phys. Chem. **100**, 170 (1996).
[12] A. J. Meixner, A. Renn, and U. P. Wild, J. Chem. Phys. **91**, 6728 (1989).
[13] K. Holliday, M. Croci, E. Vauthey, and U. P. Wild, Phys. Rev. B **47**, 14 741 (1993).
[14] M. D. Fayer, Annu. Rev. Phys. Chem. **33**, 63 (1982).
[15] T. D. Dreier and D. J. Rakestraw, Appl. Phys. B **50**, 709 (1990).
[16] M. A. Buntine, D. W. Chandler, and C. C. Hayden, J. Chem. Phys. **96**, 1640 (1992).
[17] T. J. Buthenhoff and E. A. Rohlfing, J. Chem. Phys. **96**, 5460 (1992).
[18] G. Hall and B. J. Whitaker, J. Chem. Soc. Faraday Trans. **90**, 1 (1994).
[19] J. Morais, J. Ma, and M. B. Zimmt, J. Phys. Chem. **95**, 3887 (1991).
[20] M. Terazima and N. Hirota, J. Chem. Phys. **95**, 6490 (1991).
[21] E. Vauthey and A. Henseler, J. Phys. Chem. **99**, 8652 (1995).
[22] N. Tamai, T. Asahi, and H. Masuhara, Chem. Phys. Lett. **198**, 413 (1992).
[23] T. Asahi, N. Tamai, T. Uchida, N. Shimo, and H. Masuhara, Chem. Phys. Lett. **234**, 337 (1995).
[24] D. D. Perrin, W. L. F. Armarego, and D. R. Perrin, *Purification of Laboratory Chemicals* (Pergamon, Oxford, 1980).
[25] S. Schoof and H. Güsten, Ber. Bunsenges. Phys. Chem. **82**, 1068 (1978).
[26] H. Kogelnik, Bell Syst. Technol. J. **48**, 2909 (1969).
[27] L. Genberg, Q. Bao, S. Gracewski, and R. J. D. Miller, Chem. Phys. **131**, 81 (1989).
[28] J. D. Jackson, *Classical Electrodynamics* (Wiley, New York, 1975), p. 306.
[29] K. A. Nelson, R. Casalegno, R. J. D. Miller, and M. D. Fayer, J. Chem. Phys. **77**, 1144 (1982).
[30] E. Haselbach, E. Vauthey, and P. Suppan, Tetrahedron **44**, 7335 (1988).
[31] E. Vauthey, P. Suppan, and E. Haselbach, Helv. Chim Acta **71**, 93 (1988).